The age and origin of the Labyrinth, western Dry Valleys, Antarctica: Evidence for extensive middle Miocene subglacial floods and freshwater discharge to the Southern Ocean

Adam R. Lewis
David R. Marchant
Douglas E. Kowalewski
Department of Earth Sciences, Boston University, Boston, Massachusetts 02215, USA
Suzanne L. Baldwin
Laura E. Webb
Department of Earth Sciences, Syracuse University, Syracuse, New York 13244, USA

ABSTRACT

A 50+-km-long network of bedrock channels and scoured terrain occupies the ice-free portion of a major trough that crosses the Transantarctic Mountains in southern Victoria Land. The channels, collectively termed the Labyrinth, emerge from beneath the margin of the East Antarctic Ice Sheet (Wright Upper Glacier) and are incised into a 300-m-thick sill of Ferrar Dolerite at the head of Wright Valley. Upper- and intermediate-elevation erosion surfaces of the Labyrinth exhibit striations and molding characteristic of glacial erosion. Channels and canyons on the lower surface are as much as 600 m wide and 250 m deep, have longitudinal profiles with many reverse gradients, and contain potholes >35 m deep at tributary junctions. These characteristics are most consistent with incision from fast-flowing subglacial meltwater; estimated discharge is on the order of 1.6–2.2 × 10^6 m^3s^{-1}. Our $^{40}Ar/^{39}Ar$ analyses of volcanic tephra from the Labyrinth show that the channels are relict, that major channel incision predates 12.4 Ma, and that the last major subglacial flood occurred sometime between 14.4 Ma and 12.4 Ma. The most plausible origin for the Labyrinth is erosion associated with episodic drainage of subglacial lakes in East Antarctica. One compelling possibility is that discharge of large volumes of subglacial meltwater to the Southern Ocean, and to the Ross Sea in particular, may have coincided with, and contributed to, oscillations in regional and/or global climate during the middle Miocene.

Keywords: Antarctica, Miocene, Labyrinth, subglacial floods, climate.

INTRODUCTION

During the middle Miocene, the East Antarctic Ice Sheet evolved from a dynamic and temperate state (Naish et al., 2001) to its present sluggish and extensively cold-based state. This thermal transformation coincided with one or more large-scale ice-sheet expansions (Denton et al., 1984; Marchant et al., 1993), when grounded and erosive ice extended well out onto the Ross Sea continental shelf (Anderson and Bartek, 1992; Bart et al., 2000). Although not required for catastrophic release of subglacial meltwater, such a thermal change and ice-sheet expansion may have set the stage for unusually large subglacial floods. Previous studies concerning the origin of the Labyrinth have considered the role of salt-weathering in a cold-desert climate (Shaw and Healy, 1977) and/or erosion from proglacial and subglacial meltwater (Smith, 1965; Warren, 1965; Cotton, 1966).

Regional Setting

Airborne-radar-echo depth sounding (ARE) inland of the Dry Valleys region shows that the Wright Valley trough, in which the Labyrinth sits, crosses the mountain crest at ~77°32′S (Calkin, 1974). The Labyrinth emerges from beneath the margin of Wright Upper Glacier and continues thereafter for ~10 km, ultimately draining into two major troughs to the north and south of the Dais (Fig. 1A). Two to fifteen kilometers east of the Dais is an extensive drift-free region (>45 km^2) that shows transverse bedrock ridges with a wavelength of ~22 m and an amplitude of 2–4 m (Fig. 2C). This exposed bedrock appears similar to undulating bedrock surfaces that Denton and Sugden (2005) ascribed to subglacial meltwater erosion beneath a thick East Antarctic Ice Sheet. About 75 km east of the Dais, the mouth of Wright Valley is submerged beneath a coastal piedmont glacier. ARE analyses show a 5-km-wide east-to-west–trending trough that occupies the valley axis and descends seaward, reaching a depth of more than 200 m below present sea level at ~77°23′S, 163°30′E (Calkin, 1974).

RESULTS

Labyrinth

We differentiate an upper-, intermediate-, and lower-elevation erosion surface on the Labyrinth (Fig. 1B). Each surface occupies a specific elevation range (Fig. 1C). The surfaces and incised channels are cut into a resistant and generally flat-lying (3°W dip) sill of Ferrar Dolerite. This sill is broken by two dominant near-vertical sets of joints, oriented 003° and 093° (Fig. 1E). A third set of subhorizontal joints lies parallel with the ground surface. In otherwise coherent bedrock, the joints commonly intersect to form tabular blocks ~10 cm thick and cubic forms as much as ~1.8 m on each side.

Upper Surface. The upper surface of the Labyrinth (ES1, Figs. 1B and 2B) exhibits shallow channels from 50 to 200 m wide and from 10 to 40 m deep. Striated bedrock can be found beneath isolated outcrops of coarse debris (<1 m thick). These striations, along with small-scale stoss-and-lee features (<1 m), indicate down-valley glacial flow at ~083° to 111°. The patchy debris is composed of alternating layers of coarse-grained sand and pea-sized gravel (Fig. 3). Abraded volcanic minerals and glass shards occur admixed within these sediments.

Intermediate Surface. The intermediate surface occupies platforms along the north and south walls of Wright Valley and additionally includes four small outliers near the center of the Labyrinth (ES2, Figs. 1B and 2B). Channels on this surface trend oblique to Wright Valley (060°), are up to 200 m wide and 50 m deep, and truncate the upper surface. They coalesce to form a weak dendritic pattern; drainage density (*D*) is ~1.2 km/km^2 (Figs. 1B and 1C). Some channels terminate abruptly at the base of the north valley wall, though others turn eastward and continue down the valley axis. Evidence for direct glacial erosion is restricted to the tops of interfluves and includes whale-back landforms and weakly developed striations. Stratified sediment is sparse and relatively coarse grained. Soil excavations ($n = 32$) show a gravelly basal layer with angular, imbricated cobbles (Fig. 3); on average, the largest of these imbricated cobbles measures ~40 cm long, ~30 cm wide, and ~10 cm thick; all are rip-up clasts, with sizes commensurate with small-scale jointing in underlying Ferrar Dolerite. Striations on these rip-up clasts are preserved on a single side, most likely representing the former bed-

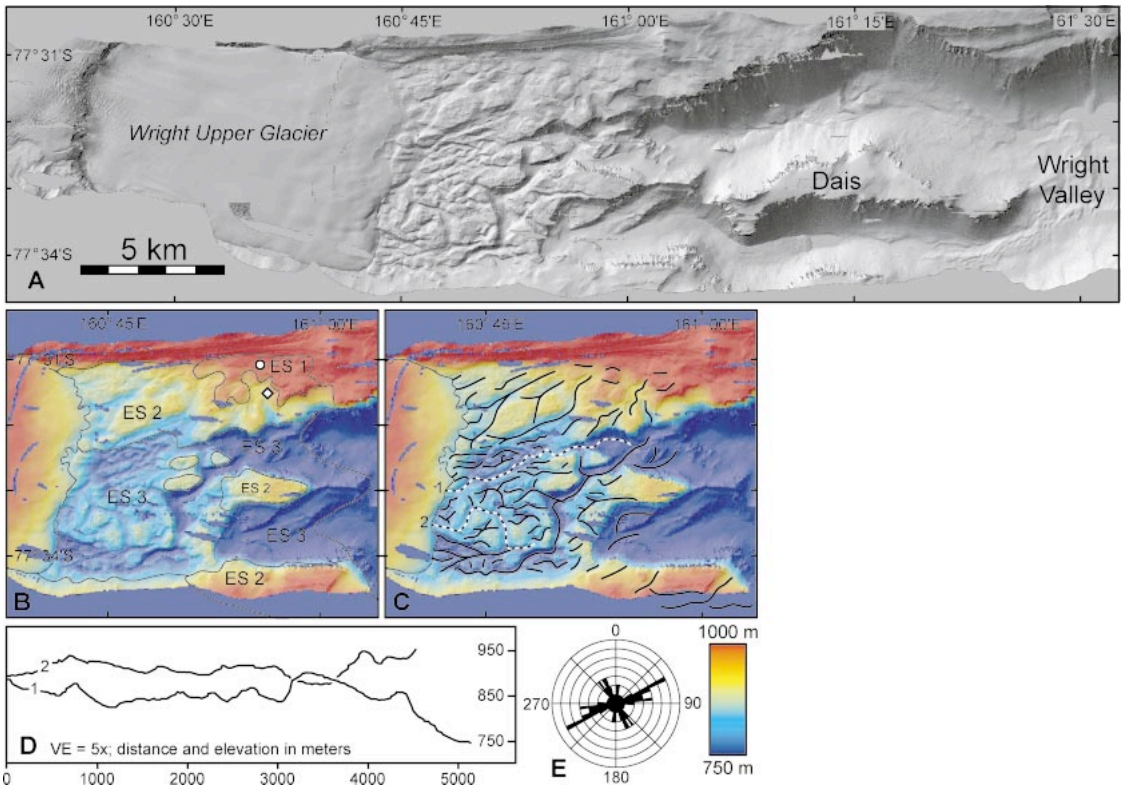

Figure 1. Digital elevation models (DEMs) of Labyrinth; data are from National Aeronautics and Space Administration laser survey mission of Dry Valleys region (with post-processing completed at Ohio State University and Brown University); north is to top, scale bar is applicable to all DEMs. A: Shaded relief DEM of Wright Upper Glacier, the Labyrinth, and Wright Valley. B: Erosion surfaces (ES) comprising the Labyrinth; circle indicates location of sample of in situ ash fall (ALS 00–102); diamond indicates location of ash reworked in stratified sediment (ALS 00–145B). C: Channels depicted as black lines and location of longitudinal profiles (1 and 2) as dashed lines. D: Longitudinal profiles for channels 1 and 2 indicated in C. E: Joint orientations displayed on rose diagram (*n* = 45 measured joints) match trends in channel orientation. VE–vertical exaggeration.

rock surface. Also common are gravelly layers of tabular cross-beds, 0.35–0.75 m thick; inferred flow directions are to the northeast, parallel with channel axes.

Lower Surface. The lower surface (ES3) occupies ~75% of the total area of the Labyrinth (Figs. 1B and 2A). It exhibits east-west–trending, anastomosing channels and canyons that truncate ES2. U-shaped canyons are up to 600 m wide and 250 m deep and *D* = ~1.8 km/km^2. The tops of most interfluves are flat, though some exhibit bedrock steps and streamlined forms reminiscent of scour by high-velocity floods (Kor et al., 1991); all interfluves are cliffed (Fig. 2A). Longitudinal-

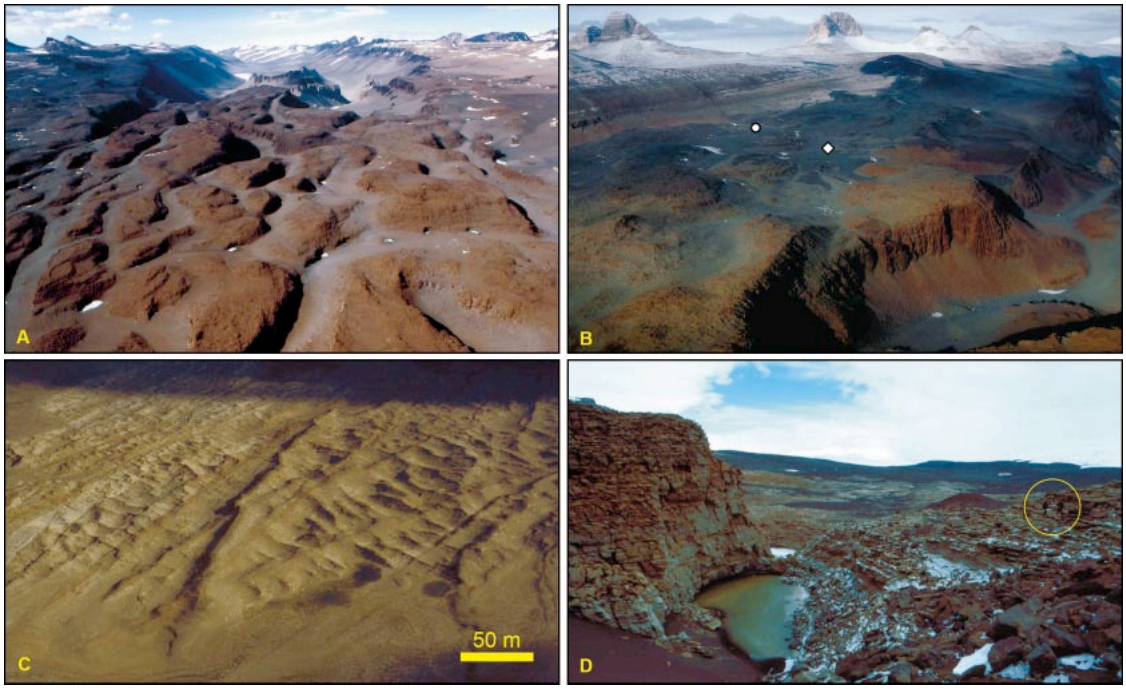

Figure 2. A: Oblique-aerial view of channels incised into lower surface (ES3) of Labyrinth; channels in foreground are ~100 m wide; main trough of Wright Valley is in background. B: Oblique-aerial view of ES1 and ES2 with deep crosscutting channel of ES3 in foreground. Irregular dark patches on ES1 and ES2 are scattered deposits of stratified sand and gravel; circle and diamond (1.2 km apart) show locations of in situ (ALS-00–102) and reworked ash (ALS-00–145B), respectively. C: Low-elevation aerial view of scoured-bedrock terrain in central Wright Valley; λ = ~22 m, with amplitudes of ~2–4 m (see text); mafic dikes cut obliquely across this corrugated, granitic bedrock. D: Oblique-aerial view of a 50-m-wide pothole incised into sandstone bedrock, Convoy Range; scoured bedrock terrain is in background. Geologists are circled for scale.

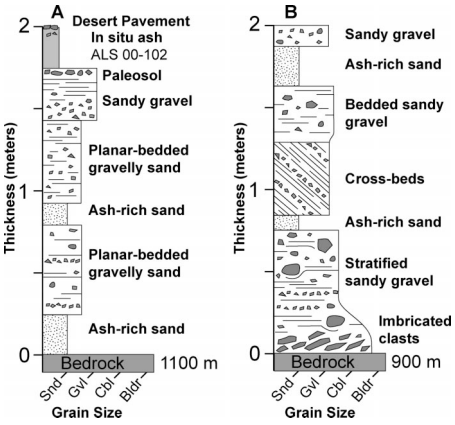

Figure 3. Generalized stratigraphic columns for stratified sediment on the (A) upper (ES1) and (B) intermediate (ES2) surfaces of Labyrinth. Snd—sand; Gvl—gravel; Cbl—cobble; Bldr—boulder; these represent maximum grain size for mapped units.

channel profiles show reverse gradients with a maximum relief of 80 m (Fig. 1D). Potholes up to 30 m in diameter occur at tributary junctions and in the lee of transverse bedrock steps; undercutting occurs at outer channel walls in tight hairpin turns. For the most part, tributary channels are not graded to the main channel system and some terminate abruptly in overdeepened hollows (e.g., ''blind terminations'' of Lowe and Anderson, 2003).

In Situ Volcanic Ash Fall. An in situ ash fall that rests on top of a buried soil on ES1 contains angular glass shards, <3% nonvolcanic grains, and displays a coherent trace-element geochemical signature (ALS 00–102, Fig. DR1[1]). The deposit occurs as a near-continuous layer, from 30 to 50 cm thick, and extends laterally for 10–20 m; it is overlain by a well-developed gravel pavement. Following Marchant et al. (1993, 1996), at least the lowermost 5 cm is believed to represent direct ash fall into a preexisting topographic hollow. The uniform geochemical signature for glass shards, the lack of evidence for mechanical abrasion, and the high concentration of ash are all consistent with ash-fall deposition. Syndepositional slumping of adjacent ash-rich diamictons (mixtures of ash and colluvium on nearby 10° to 25° slopes) most likely covered the ash fall. Deflation of this upper ash-rich diamicton probably produced the pavement that now protects the in situ ash below (e.g., Marchant et al., 1993).

Chronology

Our $^{40}Ar/^{39}Ar$ laser total fusion analyses on sanidines from the in situ ash fall (ALS-00–102) and reworked ash fall (ALS-00–145B) from the upper (ES1) and intermediate (ES2) surfaces, provide constraints on the timing of Labyrinth incision. Four $^{40}Ar/^{39}Ar$ laser total fusion analyses on aliquots of 2–4 sanidine crystals from the in situ ash fall yielded a mean age of 12.37 ± 0.66 Ma (Table DR1[1]). Because this in situ ash fall could not have been preserved beneath overriding wet-based ice, its radiometric date provides a minimum age for the Labyrinth. The age of reworked ash fall found within stratified deposits on channels of the intermediate surface can be used to help provide a maximum age for one meltwater event. Five $^{40}Ar/^{39}Ar$ laser total fusion analyses on aliquots of 2–3 sanidine crystals from this reworked ash fall (e.g., ALS-00–145B) provide a mean age of 14.36 ± 0.43 Ma. Combining these radiometric data, we argue that the last meltwater event to carve the Labyrinth occurred sometime between ca. 14 Ma and ca. 12 Ma.

DISCUSSION

Incision of the Labyrinth

The cross-cutting relationships among channels of the labyrinth show that incision likely progressed sequentially from ES1 to ES3. Each surface was cut at a time when thick, wet-based ice converged at the head of Wright Valley and flowed eastward down the valley axis. The striations and whale-back landforms found on ES1 and ES2 indicate direct erosion beneath wet-based glacial ice. For ES3, the anastomosing and U-shaped channels with reverse gradients; the bedrock steps with lee-side potholes; the hanging tributaries; and the potholes at most tributary junctions all reflect erosion from high-velocity subglacial meltwater. During incision of ES3, (and perhaps of ES2), subglacial meltwater was likely pirated to new and evolving ever-lower-elevation outlets, with each new channel increasing in size downstream from west to east (Fig. 1A). The repetitive bedrock corrugations of central Wright Valley and the deep trough leading offshore are consistent with the possibility of continued erosion of weathered bedrock by subglacial meltwater. Corroborating evidence for these large floods may be found in large-scale, offshore deltas, though subsequent erosion beneath grounded ice in the Ross Sea might have obliterated and/or masked such unconsolidated deposits (Anderson and Bartek, 1992; Bart et al., 2000).

Hydraulic plucking and abrasion from bedload and suspended load are two candidate processes that likely modified the channels on ES2 and produced those on ES3 (e.g., Hancock et al., 1998; Whipple et al., 2000). Based on the size of rip-up clasts imbedded in stratified sediment on ES2, water flow there reached at least 1–2 m/s (e.g., Costa, 1983). If we assume that meltwater entrained and transported cubic-shaped blocks of Ferrar Dolerite that were ~1.8 m on a side (a prominent block size delineated by cross-cutting joints observed on channel walls), then flow velocities during incision of ES3 could have been on the order of 11 m/s to 15 m/s. Given 1.4 × 10^5 m^2 as our cross-sectional measure for channels on ES3, our maximum estimated discharge is ~1.6–2.2 × 10^6 m^3s^{-1}. This estimate assumes ice-bed decoupling only occurred in the channels; had ice decoupled from interfluves on ES3, then discharge could have increased substantially. We postulate that the dearth of sediment in channels and in central Wright Valley reflects transport from extreme flows and/or subsequent freeze-on beneath overriding ice. Lastly, small-scale S-forms, such as spindle flutes, hairpin furrows, and other scour marks with sharp upper rims, typical of high-velocity flow separation and horseshoe vortices, are not found on channel floors and walls. Such S-forms, which are generally <2 m in size, fall below the resolution of this study; additionally, salt-weathering and wind deflation operating on exposed bedrock over the time scales considered here are capable of masking and/or obliterating such features.

Regional Correlation

The Labyrinth is one of a series of large channel networks that cross the Transantarctic Mountains (e.g., Sugden and Denton, 2004; Denton and Sugden, 2005). The largest network occurs in the Convoy Range (40 km north of the Labyrinth), where channels and potholes covering a tract at least 50 km in length emerge from beneath the margin of the East Antarctic Ice Sheet and head seaward toward the Ross Embayment. Potholes in this system are up to 40 m deep and 140 m wide (Sugden and Denton, 2004) (Fig. 2D). Lowe and Anderson (2003) mapped similar bedrock channels produced beneath an expanded West Antarctic Ice Sheet on the continental shelf near Pine Island Bay.

Meltwater Source

Given the size of the Labyrinth, and that of other meltwater systems crossing the Transantarctic Mountains (e.g., Sugden and Denton, 2004), we follow Lowe and Anderson (2003) and conclude that it is unlikely that all of the requisite water could have been produced locally by pressure melting. As one hypothesis to test, we propose catastrophic drainage of one or more inland subglacial lakes (see Dowdeswell and Siegert, 1999; Studinger et al., 2004, Siegert, 2005; and Priscu et al., 2005, for identification of existing subglacial lakes in the Ross drainage area). Estimates for the total volume of meltwater now stored in subglacial lakes beneath the East Antarctic Ice Sheet in the Ross drainage area range from ~4000 to ~10,000 km^3. The latter exceeds the volume of meltwater released to

[1]GSA Data Repository item 2006102, trace-element geochemistry and $^{40}Ar/^{39}Ar$ analyses of volcanic ashes, is available online at www.geosociety.org/pubs/ft2006.htm, or on request from editing@geosociety.org or Documents Secretary, GSA, P.O. Box 9140, Boulder, CO 80301-9140, USA.

the North Atlantic Ocean from Glacial Lake Agassiz (a proglacial lake at the margin of the Laurentide Ice Sheet) at the onset of the Younger Dryas cold period (Teller et al., 2002; Teller and Leverington, 2004). The number and total volume of subglacial lakes beneath the East Antarctic Ice Sheet in middle Miocene time could have been considerably greater than today, because at that time, the East Antarctic Ice Sheet was predominantly wet-based (Marchant et al., 1993; Sugden and Denton, 2004) and was considerably larger (Denton et al., 1984; Bart et al., 2000). Although it is impossible to estimate with accuracy the exact configuration of the East Antarctic Ice Sheet and underlying bedrock terrain for the middle Miocene, adverse slopes along the western flank of the Transantarctic Mountains (Calkin, 1974) would most likely have provided the requisite glaciological conditions for subglacial meltwater ponding (e.g., Clarke et al., 2005). In addition, the East Antarctic Ice Sheet margin would have become frozen to the substrate early as the climate cooled, and this would have provided a frozen-ice dam susceptible to episodic failure (e.g., Clarke et al., 2005). The cross-cutting channels and erosion surfaces of the Labyrinth call for repeated failure of such an ice dam and multiple discharge events.

Implications for Middle Miocene Climate Change

Results of recent climate modeling show the sensitivity of meltwater release from Antarctica to regional and global climate (Mikolajewicz, 1998; Weaver et al., 2003). Meltwater draining through the Labyrinth, the Convoy Range, and other regions in Victoria Land, would ultimately flow into the Ross Embayment, a region now critical for deep-water formation and one shown in modeling studies to be sensitive to freshwater discharge (Weaver et al., 2003). For the purposes of this discussion, we assume that during the middle Miocene some component of deep water also formed in this region.

Given a larger-than-present East Antarctic Ice Sheet and one with melting ice margins terminating on the continental shelf, local ocean salinity may have been preconditioned such that any significant addition of fresh water could have exceeded a threshold and impacted deep-water formation (e.g., Mikolajewicz, 1998; Mackensen, 2004). If this scenario is correct, then meltwater released from beneath the East Antarctic Ice Sheet, for which we have presented here geomorphic evidence for at least one (and most likely multiple) large floods between ca. 12 Ma and ca. 14 Ma (and most likely earlier as well), could be a contributing factor in the evolution of deep-water circulation and the Antarctic cryosphere; as one idea, these types of subglacial floods could potentially have served as a trigger for some recorded changes in middle Miocene climate (e.g., Zachos et al., 2001).

ACKNOWLEDGMENTS

This research was supported by U.S. National Science Foundation grants OPP-9811877, OPP-0338291 (Marchant), and EAR-IF-9725891 (Baldwin). We thank Roger LeB. Hooke for helpful and detailed comments on an earlier version of this manuscript. Reviews from John Anderson, John Priscu, and an anonymous reviewer also greatly improved this manuscript.

REFERENCES CITED

Anderson, J.B., and Bartek, L.R., 1992, Cenozoic glacial history of the Ross Sea revealed by intermediate resolution seismic reflection data combined with drill site information, *in* Kennett, J.P., ed., Antarctic Research Series, Volume 56: Washington, D.C., American Geophysical Union, p. 231–263.

Bart, P.J., Anderson, J.B., Trincardi, F., and Shipp, S.S., 2000, Seismic data from the Northern Basin, Ross Sea record multiple expansions of the East Antarctic Ice Sheet during the late Neogene: Marine Geology, v. 166, p. 31–50.

Calkin, P.E., 1974, Subglacial geomorphology surrounding the ice-free valleys of southern Victoria Land, Antarctica: Journal of Glaciology, v. 13, p. 415–429.

Clarke, G.K.C., Leverington, D.W., Teller, J.T., and Dyke, A.S., 2005, Fresh arguments against the Shaw megaflood hypothesis: A reply to comments by David Sharpe on ''Paleohydraulics of the last outburst flood from glacial Lake Agassiz and the 8200 B.P. cold event'': Quaternary Science Reviews, v. 24, p. 1533–1541, doi: 10.1016/j.quascirev.2004.12.003.

Costa, J.E., 1983, Paleohydraulic reconstruction of flash-flood peaks from boulder deposits in the Colorado Front Range: Geological Society of America Bulletin, v. 94, p. 986–1004, doi: 10.1130/0016-7606(1983)94<986:PROFPF>2.0.CO;2.

Cotton, C.A., 1966, Antarctic scablands: New Zealand Journal of Geology and Geophysics, v. 9, p. 130–132.

Denton, G.H., and Sugden, D.E., 2005, Meltwater features that suggest Miocene ice-sheet overriding of the Transantarctic Mountains in Victoria Land, Antarctica: Geografiska Annaler, v. 87A, p. 67–85.

Denton, G.H., Prentice, M.L., Kellogg, D.E., and Kellogg, T.B., 1984, Late Tertiary history of the Antarctic ice sheet: Evidence from the Dry Valleys: Geology, v. 12, p. 263–267, doi: 10.1130/0091-7613(1984)12<263:LTHOTA>2.0.CO;2.

Dowdeswell, J.A., and Siegert, M.J., 1999, The dimensions and topographic setting of Antarctic subglacial lakes and implications for large-scale water storage beneath continental ice sheets: Geological Society of America Bulletin, v. 111, p. 254–263, doi: 10.1130/0016-7606(1999)111<0254:TDATSO>2.3.CO;2.

Hancock, G.S., Anderson, R.S., and Whipple, K.X, 1998, Beyond power: Bedrock river incision process and form, *in* Tinkler, K.J., and Wohl, E.E., eds., Rivers and rock: American Geophysical Union Geophysical Monograph 107, p. 35–60.

Kor, P.S.G., Shaw, J., and Sharpe, D.R., 1991, Erosion of bedrock by subglacial meltwater, Georgian Bay, Ontario: A regional view: Canadian Journal of Earth Sciences, v. 28, no. 4, p. 623–642.

Lowe, A.L., and Anderson, J.B., 2003, Evidence for abundant subglacial meltwater beneath the paleo-ice sheet in Pine Island Bay, Antarctica: Journal of Glaciology, v. 49, p. 125–138.

Mackensen, A., 2004, Changing Southern Ocean palaeocirculation and effects on global climate: Antarctic Science, v. 16, p. 369–386, doi: 10.1017/S0954102004002202.

Marchant, D.R., Denton, G.H., Sugden, D.E., and Swisher, C.C., III, 1993, Miocene glacial stratigraphy and landscape evolution of the western Asgard Range, Antarctica: Geografiska Annaler, v. 75A, p. 303–330.

Marchant, D.R., Denton, G.H., Swisher, C.C., III, and Potter, N.P., Jr., 1996, Late Cenozoic Antarctic paleoclimate reconstructed from volcanic ashes in the Dry Valleys region of Southern Victoria Land: Geological Society of America Bulletin, v. 108, p. 181–194, doi: 10.1130/0016-7606(1996)108<0181:LCAPRF>2.3.CO;2.

Mikolajewicz, U., 1998, Effect of meltwater input from the Antarctic ice sheet on the thermohaline circulation: Annals of Glaciology, v. 27, p. 311–315.

Naish, T.R., and 32 others, 2001, Orbitally induced oscillations in the East Antarctic Ice Sheet at the Oligocene/Miocene boundary: Nature, v. 413, p. 719–723.

Priscu, J.C., Kennicutt, M.C., Bell, R.E., Bulat, S.A., Ellis-Evans, J.C., Lukin, V.V., Petit, J.-R., Powell, R.D., Siegert, M.J., and Tabacco, I., 2005, Exploring subglacial Antarctic lake environments: Eos (Transactions, American Geophysical Union), v. 86, no. 20, p. 193–197.

Siegert, M.J., 2005, Lakes beneath the ice sheet: The occurrence, analyses, and future exploration of Lake Vostok and other Antarctic subglacial lakes: Annual Reviews of Earth and Planetary Science, v. 33, p. 215–245, doi: 10.1146/annurev.earth.33.092203.122725.

Shaw, J., and Healy, T.R., 1977, The formation of the Labyrinth, Wright Valley, Antarctica: New Zealand Journal of Geology and Geophysics, v. 20, p. 933–947.

Smith, H.T.U., 1965, Anomalous erosional topography in Victoria Land: Antarctic Science, v. 148, p. 941–942.

Studinger, M., Bell, R.E., and Tikku, A.A., 2004, Estimating the depth and shape of subglacial Lake Vostok's water cavity from aerogravity data: Geophysical Research Letters, v. 31, no. L12401, doi: 10.1029/2004GL019801.

Sugden, D., and Denton, G., 2004, Cenozoic landscape evolution of the Convoy Range to MacKay Glacier area, Transantarctic Mountains: Onshore to offshore synthesis: Geological Society of America Bulletin, v. 116, p. 840–857.

Teller, J.T., and Leverington, D.W., 2004, Glacial Lake Agassiz: A 5000-year history of change and its relationship to the delta 18-O record of Greenland: Geological Society of America Bulletin, v. 116, p. 729–742, doi: 10.1130/B25316.1.

Teller, J.T., Leverington, D.W., and Mann, J.D., 2002, Freshwater outbursts to the oceans from glacial Lake Agassiz and their role in climate change during the last deglaciation: Quaternary Science Reviews, v. 21, no. 8–9, p. 879–887, doi: 10.1016/S0277-3791(01)00145-7.

Warren, C.R., 1965, Wright Valley: Conjectural volcanoes: Science, v. 149, p. 658.

Weaver, A.J., Saenko, O.A., Clark, P.U., and Mitrovica, J.X., 2003, Meltwater pulse 1A from Antarctica as a trigger of the Bølling-Allerod warm interval: Science, v. 299, p. 1709–1713, doi: 10.1126/science.1081002.

Whipple, K.X, Hancock, G.S., and Anderson, R.S., 2000, River incision into bedrock: Mechanics and relative efficacy of plucking, abrasion, and cavitation: Geological Society of America Bulletin, v. 112, p. 490–503, doi: 10.1130/0016-7606(2000)112<0490:RIIBMA>2.3.CO;2.

Zachos, J.C., Pegani, M., Stone, L., Thomas, E., and Billups, K., 2001, Trends, rhythms, and aberrations in global climates 65 Ma to present: Science, v. 292, p. 686–693, doi: 10.1126/science.1059412.

Manuscript received 8 August 2005
Revised manuscript received 26 January 2006
Manuscript accepted 2 February 2006

Printed in USA